35th Annual International Conference of the IEEE EMBS
Osaka, Japan, 3 - 7 July, 2013

Selection and Control of Limb Posture for Stability*

David W. Franklin, Luc P.J. Selen, Sae Franklin, and Daniel M. Wolpert

Abstract— **Impedance control can be used to stabilize the limb against both instability and unpredictable perturbations. Limb posture influences motor noise, energy usage and limb impedance as well as their interaction. Here we examine whether subjects use limb posture as part of a mechanism to regulate limb stability. Subjects performed stabilization tasks while attached to a two dimensional robotic manipulandum which generated a virtual environment. Subjects were instructed that they could perform the stabilization task anywhere in the workspace, while the chosen postures were tracked as subjects repeated the task. In order to investigate the mechanisms behind the chosen limb postures, simulations of the neuro-mechanical system were performed. The results indicate that posture selection is performed to provide energy efficiency in the presence of force variability.**

I. Introduction

The sensorimotor control system produces skillful movements despite the problems of noise, uncertainty, delays and nonlinearities in the system. One of the computational mechanisms that ameliorates these problems is impedance control [1]. For example, when subjects interact with an unstable environment, they learn to selectively control the stiffness of their arm to adapt to the environment [2-4]. This adaptation of endpoint stiffness is modulated to trade off mechanical stability with the destabilizing effects of signal-dependent noise [5]. However the limb impedance can be modulated both by co-contraction and by changing the limb posture [6]. Any change in limb posture directly influences the passive endpoint stiffness of the arm [7], the inertial properties of the arm [6], the ability to manipulate stiffness [8], the ability to stabilize perturbations [9], and the effects of motor and sensory noise [10]. However, only recently have studies started to investigate the influence of arm posture on human motor control. Specifically it has been shown that when subjects are in unstable environments, they orient their arm so that the passive stiffness is large along the direction of instability [11]. Similarly it has been demonstrated that the variability of the endpoint of movements is strongly influenced by the limb geometry [12]. However, changes in limb geometry can also influence the effect of motor noise on muscle tension, joint torques and endpoint force, further complicating a stable interaction with the environment. We behaviorally tested whether humans systematically use different postures to deal with different stability requirements and developed a computational neuro-mechanical model of the arm to interpret the results.

*Research supported by the Wellcome Trust.

D. W. Franklin is with the Computational & Biological Learning Laboratory in the Department of Engineering, University of Cambridge, Cambridge, CB2 1PZ, U.K (phone: +44 1223 748516; fax: +44 1223 765587; e-mail: dwf25@cam.ac.uk).

L.P.J. Selen is with the Donders Institute for Brain, Cognition and Behaviour, Radboud University Nijmegen, 6500HB Nijmegen, The Netherlands (e-mail: l.selen@donders.ru.nl).

S. Franklin is with the Computational & Biological Learning Laboratory in the Department of Engineering, University of Cambridge, Cambridge, CB2 1PZ, U.K (e-mail: sf394@cam.ac.uk).

D. M. Wolpert is with the Computational & Biological Learning Laboratory in the Department of Engineering, University of Cambridge, Cambridge, CB2 1PZ, U.K (e-mail: wolpert@eng.cam.ac.uk).

II. Experimental Methods

A. Subjects

Sixteen subjects (4 female) aged 24.1±5.0 years participated in the experiments. All subjects were right-handed according to the Edinburgh handedness inventory with no reported neurological disorders. Subjects gave informed consent and the institutional ethics committee approved the experiments.

B. Experimental Setup

Subjects interacted with simulated rigid objects in the horizontal plane, approximately 10 cm below the subjects' shoulder level. The forearm was supported against gravity with an air sled. The subject grasped the handle of a robotic manipulandum (vBOT, [13]) that was used to generate the environmental dynamics (Fig. 1A). Position and force data were sampled at 1KHz. Endpoint forces at the handle were measured using an ATI Nano 25 6-axis force-torque transducer (ATI Industrial Automation, NC, USA). Visual feedback was provided using an LCD monitor and mirror mounted above the vBOT. This virtual reality system covers the manipulandum, arm and hand of the subject preventing any visual information of their location. The subjects' hand was attached to the handle of the vBOT using a thermoplastic cuff, which limited movement of the wrist and constrained the subjects' movement to only elbow and shoulder motion (subjects' trunks were fixed in the seat using a racing harness). The shoulder position and limb segment lengths were measured for each subject.

C. Protocol

Subjects performed an interaction task in which they were required to push a virtual disk attached to their hand (orange, Fig. 1B) against a frictionless circular object (blue, Fig. 1B) of varying size and hence stability. The required force was 6 ± 0.5 N in one of four directions (Fig. 1C). A successful trial involved the subject producing the desired force magnitude and direction for two seconds. Three different stability levels were examined: a fully stable object (the disk was attached by a stiff spring to the object), a moderately unstable object and a highly unstable object (Fig. 1B). The instability was determined by the size of the circular object (0.75 or 0.35 cm radii). Twenty trials of the same condition (stability level and force direction) were presented sequentially with subjects free to re-position their arm between trials (and hence the object, which was placed next to the hand) so that they could choose where to perform the task within the workspace. The order of conditions was randomly chosen, and each new condition started with one of three initial limb postures (far left, far right, near middle). Each condition, i.e., stability level and force direction, was presented three times throughout the experiment (once for each possible starting position). In order to avoid the confounding effects of visual feedback location, the visual feedback (hand, object and force vector) on each trial was presented randomly at one of 20 different locations (hence there was a translation between visual and actual hand location). The final five trials, out of 20, in each condition were used as representative of where the subjects preferred to perform the task.

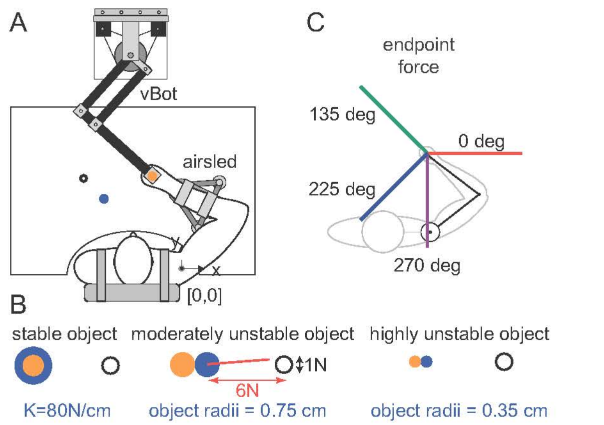

Figure 1. Experimental design. A) The setup of the robotic manipulandum. B) Three tasks of varying stability demands. The hand (orange circle) produced a force onto the fixed object (blue circle). The exerted force (red line) was required to be maintained within the 6 ± 0.5 N force target (black circle) for 2 seconds for a successful trial. All objects were visible to the subjects. C) Forces were produced in four directions.

III. Computational Simulations

In order to examine the mechanisms that govern the choice of the particular postures chosen in our tasks, we developed a model of the neuro-muscular system of the arm.

A. Model Details

The arm was modeled as a two-link system exerting an endpoint force onto a rigid frictionless circular object similar to the experimental design. The arm model was driven by six muscles (Fig. 2). These muscles were comprised of two single joint elbow muscles, two single joint shoulder muscles and two biarticular muscles. Endpoint force (**F**) was calculated as:

$$\mathbf{F} = \left(\mathbf{J}^T\right)^{-1} \mathbf{D}^T \mathbf{F}_m \tag{1}$$

where $\mathbf{D}^T$ is the 6 x 2 matrix of moment arms (equal sizes for all muscles), $\mathbf{F}_m$ is the matrix of muscle forces, and **J** is the limb Jacobian. The joint stiffness (**R**) was calculated as:

$$\mathbf{R} = \mathbf{R}_{base} + \mathbf{D}^T c_m \mathbf{F}_m \mathbf{D} \tag{2}$$

where c_m is the stiffness constant (75 m^{-1}), and $\mathbf{R}_{base}$ is the passive joint stiffness ([10.8 2.83; 2.51 8.67] Nm/rad) as obtained from [14]. The activation of each muscle was contaminated with signal dependent noise, using values that produced similar levels (3% coefficient of variability) of variability in endpoint force to those measured experimentally [15,16]. Together, this meant that both muscle stiffness and motor noise scaled linearly with the muscle activation [5].

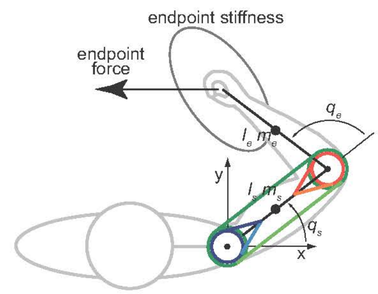

Figure 2. The six muscle, two joint model of the human arm. The endpoint stiffness of the limb depends on the limb posture and the particular set of muscle activations that produce the required endpoint force.

B. Model Properties

The model was compared to experimental results. Similar to previous studies of passive endpoint limb stiffness [7], the model produced changes as a function of the limb posture, with the stiffness ellipse becoming more isotropic close to the shoulder (Fig. 3A). Similarly, when force was exerted in different directions in the horizontal plane, the endpoint stiffness modulated similar to previous experimental results [14] (Fig. 3B). When endpoint stiffness is modulated by changes in muscle activation, this also results in changes in the size and direction of the endpoint force variability (Fig. 3C). Modeling these changes are critical to understanding the interaction between signal dependent noise and limb impedance [5].

C. Simulations

Simulations were performed separately at each of all possible joint postures within the experimental workspace (5° tiling providing 477 limb postures). For each limb posture, and for each of the 4 force directions, the simulation was performed at a large number of different combinations of muscle activation patterns (>2000) that all produced the required endpoint force. Muscle activations were contaminated with signal-dependent noise, making some of the activation patterns unstable. In a forward simulation, these noisy forces were exerted on a two-link system with the corresponding joint stiffness matrix and external constraints set by the object curvature. The joint damping matrix was set equal to 5% of the stiffness matrix. This value is of similar magnitude to both that used in computational models of the arm [5,17] and those measured experimentally [8]. Only simulations in which the arm was able to maintain contact with the object for the entire simulation time (15 s) were considered successful.

IV. Results

A. Experimental Results

Throughout the trials subjects explored a large part of the workspace in order to find limb postures that allowed them to perform the task and/or felt comfortable. However, by the end of the twenty trials, subjects generally converged to the same location for the same task regardless of the initial posture. For each force direction and stability level, subjects chose to perform the task in systematically different locations (Fig. 4). We hypothesized that the choice of limb geometry was determined by subjects choosing the minimum energetic solution that allowed postural stabilization (i.e., subject to the interaction between motor noise and muscular stiffness).

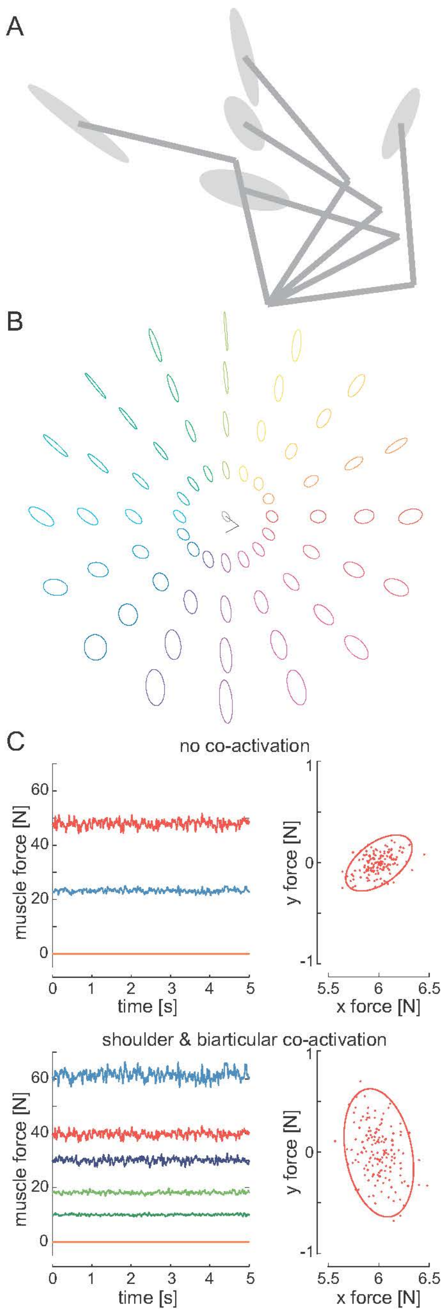

Figure 3. Properties of the neuromechanical model. A) The passive endpoint stiffness of the model as a function of limb posture. B) The model produces endpoint stiffness of the limb which modulates with endpoint force. C) Modulating the muscle co-activation produces changes in the variability of the endpoint force. Both plots show the muscle activation and endpoint force variability for the production of 6N in the positive x-axis.

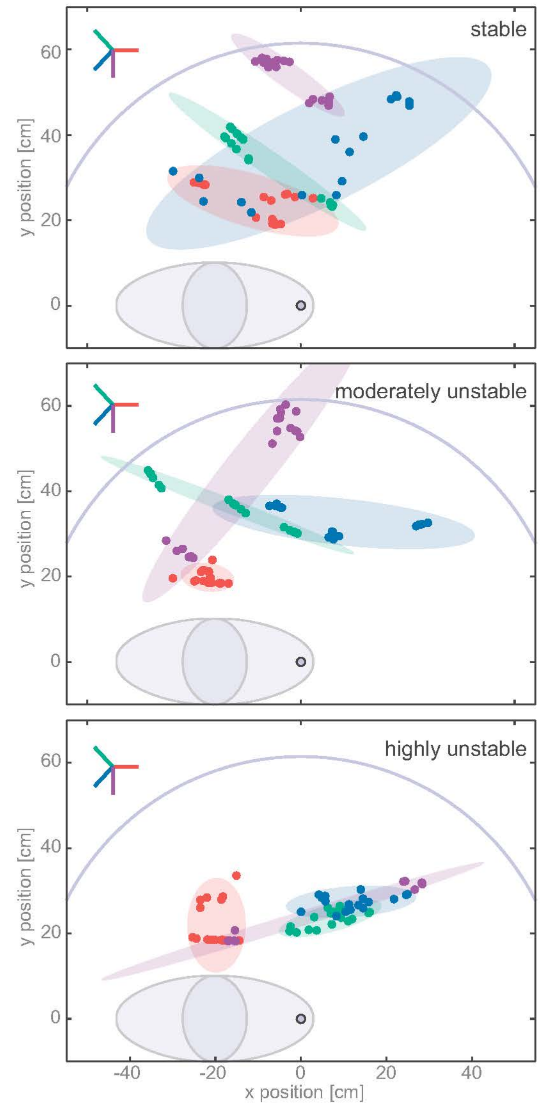

Figure 4. The final five postures chosen by a sample subject interacting with the stable, moderately unstable, and highly unstable objects. Colors indicate force direction. Shaded areas represent the 95% confidence region.

B. *Simulation Results*

The minimum muscle activation pattern that was able to maintain stability while producing the required endpoint force was found for each force direction, stability condition and posture (Fig 5A). The final postures chosen by the subjects (Fig 5, white dots show last 5 trials for all 16 subjects and all 3 repetitions) were in most cases close to the minimal muscle activation that could maintain stability, although there were exceptions for some subjects. For the most stable object, the chosen limb postures were well fit by the minimum muscle activation that could produce the desired force against the object, without any constraints on stability. Similarly, for the highly unstable object (Fig. 5B), the results were reasonably fit by the minimal muscle activation that could maintain stability against the highly unstable object.

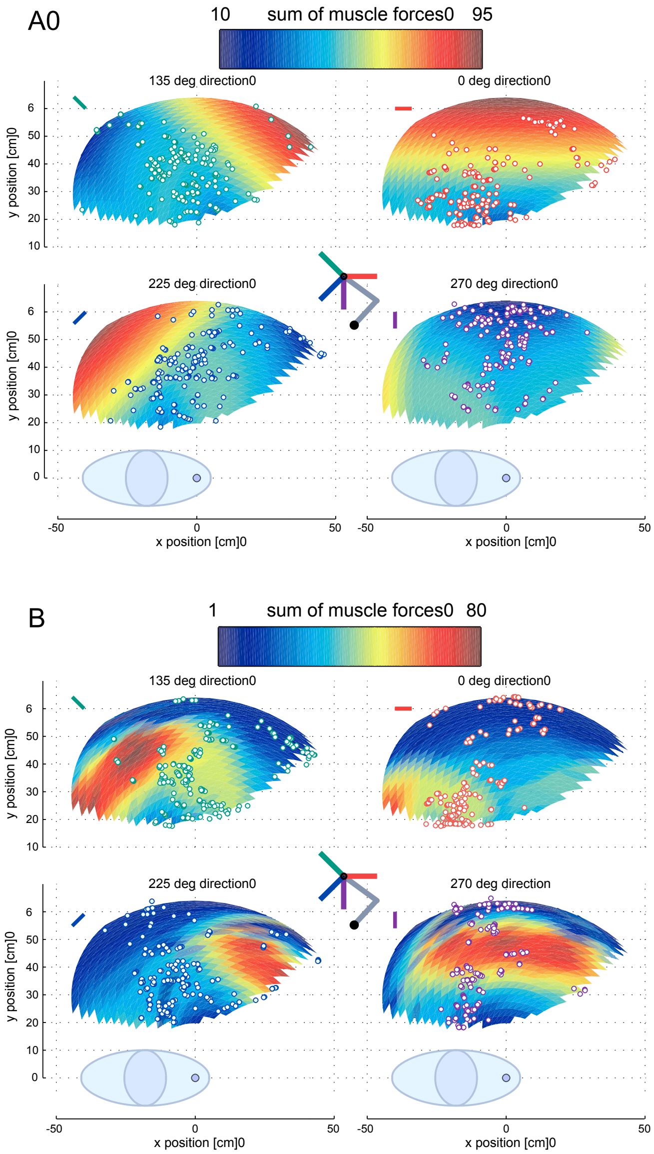

Figure 5. Simulated muscle activation patterns for successful stabilization shown with subjects' positional preferences in the workspace. A) Minimum sum of muscle activation that produces the required force in the correct direction for each posture. Overlaid white dots represent the final posture of 6 subjects in the stable object condition. B) The highly unstable object. Note the order of magnitude difference in activation between A and B.

V. Conclusion

These results of our experiments and simulations suggest that the subjects were choosing limb postures in which the muscle activation pattern could be manipulated so that endpoint stiffness ensured stability despite its concomitant force variability. However, the subjects' postures do not perfectly fit the model predictions in all cases. It is unclear whether this is because the subjects were still exploring the space of possible solutions or whether there are other costs that need to be considered within the model predictions. Specifically, the model ignores the contribution of task-dependent changes in feedback responses, which can provide additional stability [18-19]. However, despite these issues, we believe that the results suggest that posture selection is strongly related to maximizing energy efficiency in the presence of force variability and stability requirements.

Acknowledgment

We thank Ian S. Howard and James N. Ingram for their assistance with the vBOT robotic interface.

References

[1] D. W. Franklin and D. M. Wolpert, "Computational mechanisms of sensorimotor control," Neuron, vol. 72, no. 3, pp. 425–442, Nov. 2011.
[2] E. Burdet, R. Osu, D. Franklin, T. Milner, and M. Kawato, "The central nervous system stabilizes unstable dynamics by learning optimal impedance," Nature, vol. 414, no. 6862, pp. 446–449, 2001.
[3] D. W. Franklin, U. So, M. Kawato, and T. E. Milner, "Impedance control balances stability with metabolically costly muscle activation," J Neurophysiol, vol. 92, no. 5, pp. 3097–3105, Nov. 2004.
[4] D. W. Franklin, G. Liaw, T. E. Milner, R. Osu, E. Burdet, and M. Kawato, "Endpoint stiffness of the arm is directionally tuned to instability in the environment," J. Neurosci., vol. 27, no. 29, pp. 7705–7716, Jul. 2007.
[5] L. P. J. Selen, D. W. Franklin, and D. M. Wolpert, "Impedance control reduces instability that arises from motor noise," J. Neurosci., vol. 29, no. 40, pp. 12606–12616, Oct. 2009.
[6] N. Hogan, "The Mechanics of Multi-Joint Posture and Movement Control," Biol Cybern, vol. 52, no. 5, pp. 315–331, 1985.
[7] F. A. Mussa-Ivaldi, N. Hogan, and E. Bizzi, "Neural, Mechanical, and Geometric Factors Subserving Arm Posture in Humans," J. Neurosci., vol. 5, no. 10, pp. 2732–2743, 1985.
[8] E. J. Perreault, R. F. Kirsch, and P. E. Crago, "Multijoint dynamics and postural stability of the human arm," Exp Brain Res, vol. 157, no. 4, pp. 507–517, Aug. 2004.
[9] T. E. Milner, "Contribution of geometry and joint stiffness to mechanical stability of the human arm," Exp Brain Res, vol. 143, no. 4, pp. 515–519, Apr. 2002.
[10] R. van Beers, A. Sittig, and J. van der Gon, "The precision of proprioceptive position sense," Exp Brain Res, vol. 122, no. 4, pp. 367–377, 1998.
[11] R. D. Trumbower, M. A. Krutky, B.-S. Yang, and E. J. Perreault, "Use of self-selected postures to regulate multi-joint stiffness during unconstrained tasks," PLoS ONE, vol. 4, no. 5, p. e5411, 2009.
[12] D. R. Lametti and D. J. Ostry, "Postural constraints on movement variability," J Neurophysiol, vol. 104, no. 2, pp. 1061–1067, Aug. 2010.
[13] I. S. Howard, J. N. Ingram, and D. M. Wolpert, "A modular planar robotic manipulandum with end-point torque control," J. Neurosci. Methods, vol. 181, no. 2, pp. 199–211, Jul. 2009.
[14] H. Gomi and R. Osu, "Task-dependent viscoelasticity of human multijoint arm and its spatial characteristics for interaction with environments," J. Neurosci., vol. 18, no. 21, pp. 8965–8978, Nov. 1998.
[15] K. E. Jones, A. F. Hamilton, and D. M. Wolpert, "Sources of signal-dependent noise during isometric force production," J Neurophysiol, vol. 88, no. 3, pp. 1533–1544, Sep. 2002.
[16] A. F. de C. Hamilton, K. E. Jones, and D. M. Wolpert, "The scaling of motor noise with muscle strength and motor unit number in humans," Exp Brain Res, vol. 157, no. 4, pp. 417–430, Aug. 2004.
[17] D. W. Franklin, E. Burdet, K. P. Tee, R. Osu, C.-M. Chew, T. E. Milner, and M. Kawato, "CNS learns stable, accurate, and efficient movements using a simple algorithm," J. Neurosci., vol. 28, no. 44, pp. 11165–11173, Oct. 2008.
[18] M. Dimitriou, D. W. Franklin and D. M. Wolpert, "Task-dependent coordination of rapid bimanual motor responses," J Neurophysiol, vol. 107, no. 3, pp. 890-901, Feb. 2012.
[19] M. A. Krutky, V. J. Ravichandran, R. D. Trumbower, and E. J. Perreault, "Interactions between limb and environmental mechanics influence stretch reflex sensitivity in the human arm," J Neurophysiol, vol. 103, no. 1, pp. 429-440, Jan. 2010.